ELSEVIER

Journal of Nuclear Materials 246 (1997) 180–188

journal of nuclear materials

High temperature interaction between Zircaloy-4 and Inconel-718

H. Uetsuka *, F. Nagase, T. Otomo

Department of Reactor Safety Research, Japan Atomic Energy Research Institute, Tokai-mura, Ibaraki-ken, 319-11, Japan

Received 18 February 1997; accepted 24 April 1997

Abstract

The chemical interactions between Zircaloy-4 and Inconel-718 were investigated in the temperature range from 1223 to 1523 K. Multiple layers were formed at the interface of the reaction couple. The reaction generally obeyed a parabolic rate law and the rate of the reaction was determined at each examined temperature. It increased with the temperature increase. The discontinuity in the temperature dependence of the reaction rate was found at two temperatures, at about 1240 K and 1450 K. The elemental analysis with an SEM/EDX indicated that the discontinuities corresponded to the change of the reaction mechanism. © 1997 Elsevier Science B.V.

1. Introduction

Since the TMI-2 accident in 1979, many integral experiments [1–5] have been performed to investigate the degradation of fuel bundle and melt progression in a reactor core during a severe accident. The reactor core might reach very high temperatures in a severe accident. Then, core component materials chemically interact to form liquid phases that can dissolve the fuel rods far below the melting temperatures of UO_2 and Zircaloy. This enhances dissolution of UO_2 fuel, resulting in the release of a large amount of fission products.

The experiments using PWR type fuel bundles [1,2] showed that the Inconel grid spacer as well as the Ag–In–Cd alloy control rod forms liquid phases at relatively low temperatures in the course of temperature escalation and greatly influences the bundle degradation. Inconel is a nickel-base alloy and the equilibrium phase diagram of the Zr–Ni system [6] indicates the possibility of eutectic reactions between Zircaloy and Inconel at temperatures as low as 1200 K. The chemical interactions between Zircaloy and Inconel have been tested by some investigators [7–10]. Hofmann et al. [7,8] extensively investigated this reaction system at high temperatures, and reported the rates of the reaction. They are the only reaction kinetics available for the severe accident analysis. They could measure the reaction at temperatures up to 1473 K. However, the data were not obtained at 1523 K, since the specimen was completely liquefied within a short time in their experiment. For the severe accident analysis on the bundle degradation, it is very important to obtain the reaction kinetics available for a wide temperature range especially for high temperatures where the significant liquefaction occurs.

2. Materials and experimental procedure

The chemical compositions of Zircaloy-4 (Zircaloy) and Inconel-718 (Inconel) used in the present study are shown in Table 1. A reaction couple consisting of these two materials was manufactured for the isothermal annealing test. The geometry of the reaction couple is schematically shown in Fig. 1. The outer diameter of an Inconel pellet and the inner diameter of a Zircaloy crucible were the same. The Inconel pellet was pressed into the Zircaloy crucible to obtain a good contact condition at the interface. The reaction couple was isothermally heated in an infrared furnace under flowing argon. The annealing temperature ranged from 1223 to 1523 K and the annealing time ranged from 30 to 2.88×10^4 s (8 h). A rapid heat-up of 10 K/s and short-time holding at a high target temperature were programmed and successfully achieved. A Pt–Pt/13%Rh thermocouple was spot-welded on the bottom

* Corresponding author. Tel.: +81-29 282 5297; fax: +81-29 282 5323; e-mail: uetsuka@popsvr.tokai.jaeri.go.jp.

PII S0022-3115(97)00104-9

Table 1
Chemical composition of Zircaloy and Inconel-718 in wt%

Material	Sn	Fe + Cr	C	Hf	Zr	O	H	N
Zircaloy-4	1.52	0.30	0.005	< 0.005	Bal.	0.101	< 0.002	< 0.002

Material	Ni	Fe	Cr	Mo	C	Si	Mn	P	S	Cu	Al	Ti	B	Co	Nb + Ta
Inconel-718	Bal.	18.3	17.9	3.1	0.005	0.11	0.35	0.003	0.005	0.01	0.53	1.01	0.004	0.1	5.17

surface of the specimen for the temperature control and the temperature measurement. Prior to the reaction test, the temperature distribution was measured at several positions on a dummy specimen. It was shown that the temperature difference throughout a reaction couple was less than 10 K. After the isothermal annealing, the power supply to the furnace was switched off and the reaction couple was cooled in flowing argon. The cooling rate in the concerned temperature range was almost equivalent to the heating rate. Then, the reaction couple was vertically cut at its center line and, prior to metallurgical examination, the cross-section was mechanically polished and chemically etched in a solution (55 vol.% $CH_3CH(OH)COOH$, 19% HNO_3, 19% H_2O, and 7% HF). In addition, elemental analyses were performed with an SEM/EDX (scanning electron microscopy/energy dispersive X-ray spectroscopy), a Shimadzu Superscan 330FEG operating at 20kV and equipped with a Philips EDAX.

3. Results and discussion

3.1. Chemical behavior

3.1.1. Reaction at 1223 K

Fig. 2 shows the microstructure of the reaction layer formed at the interface of the reaction couple annealed at 1223 K for 1.44×10^4 s (4 h). In the reaction layer, bright and fine precipitates are observed at the Inconel side, while large precipitates are observed at the Zircaloy side. This morphology change of the precipitates suggests the concentration change of the elements in the reaction layer. As seen in the magnified photograph 'A', a very thin layer formed adjacent to the Inconel. The thicker layer adjacent to the Zircaloy is called the layer I and the thinner is called the layer II hereinafter.

The results of the quantitative elemental analysis of both the reaction layers are summarized in Table 2. The mean chemical composition of each layer obtained by integral analysis for the layer thickness is shown in the

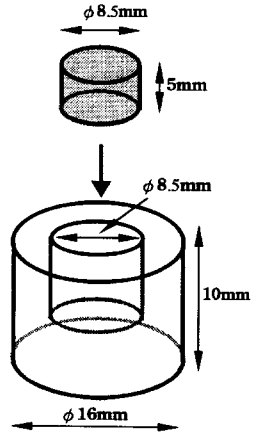

Fig. 1. Schematic illustration and geometry of the reaction couple.

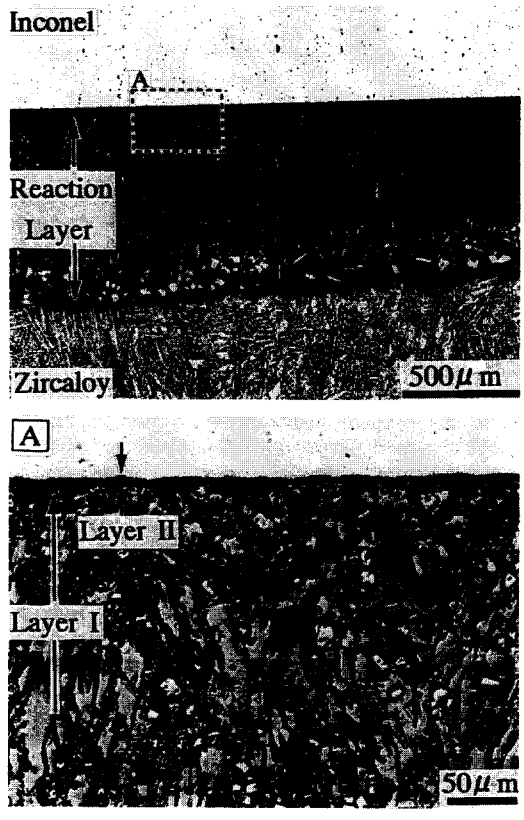

Fig. 2. Microstructure of the reaction layer of the reaction couple annealed at 1223 K for 1.44×10^4 s.

Table 2
Summary of SEM/EDX analysis of the reaction layers

Reaction temp.	Layer (position)	Composition (at.%)					Atomic ratio		
		Zr	Ni	Cr	Fe	Sn	Ni:Zr	Cr:Zr	Fe:Zr
1223 K	layer I	64	15	14	7	1	19:81	18:82	10:90
	(Zry side	71	18	4	6	1	20:80	5:95	8:92)
	(Inconel side	60	15	17	8	1	20:80	22:78	12:88)
	layer [a]	2	36	29	18	0	95: 5	94: 6	90:10
1273 K	layer I	72	18	4	5	1	20:80	5:95	6:94
	layer II [b]	37	7	34	15	0	16:84	48:52	29:71
1423 K	layer I	69	19	5	5	1	22:78	7:93	7:93
	layer II	34	8	38	18	0	19:81	53:47	35:65
	layer III [c]	7	44	21	18	0	86:14	75:25	72:28
1473 K	phase A	68	19	6	6	1	22:78	8:92	8:92
	phase B	44	20	21	15	0	31:69	32:68	25:75
	phase C	35	36	15	15	0	51:49	30:70	30:70
	phase D [d]	8	47	20	17	0	85:15	71:29	68:32

[a] The layer contains Nb + Mo + Ti of about 10 at.%.
[b] The layer contains Nb + Al + Ti of about 7 at.%.
[c] The layer contains Nb + Ti + Al of about 10 at.%.
[d] The phase contains Nb + Mo + Ti + Al of about 8 at.%.

table. The analysis showed that the layer I formed at 1223 K consisted mainly of Zr, Ni, and Cr, and the composition was estimated to be $Zr_{0.64}Ni_{0.15}Cr_{0.14}Fe_{0.07}Sn_{0.01}$. Compositions were also measured separately at the Zircaloy side and the Inconel side, since the morphology of precipitates was different in two regions. The analysis indicated apparent difference in the concentrations of Zr and Cr. The Zr concentration is higher but the Cr concentration is lower in the Zircaloy side compared to the average concentration of the total layer thickness. The atomic ratios between the main elements are also shown in the table. The Ni/Zr, Cr/Zr and Fe/Zr ratios of the layer I are 19/81, 18/82 and 10/90, respectively, and they are nearly constant throughout the reaction layer. The Zr–Ni phase diagram

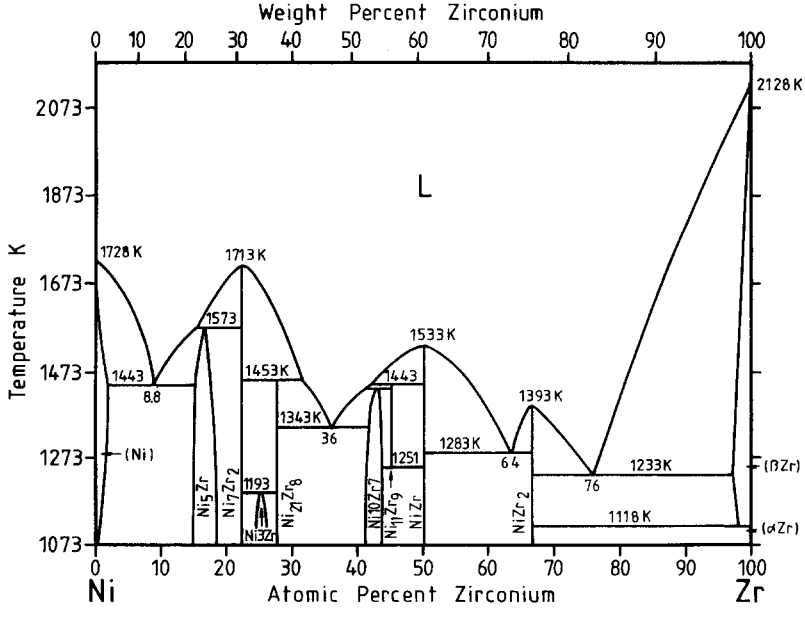

Fig. 3. Binary phase diagram of the Ni–Zr system [6].

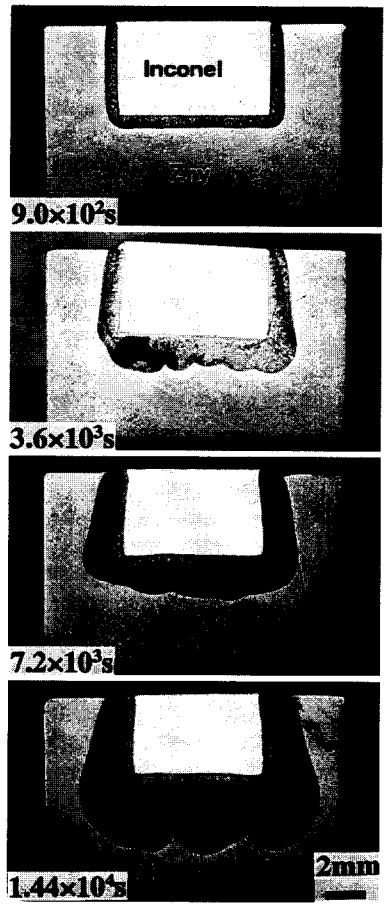

Fig. 4. Cross-sections of the reaction couples annealed at 1273 K for various times.

shown in Fig. 3 [6] indicates that the composition of such low Ni/Zr ratio is close to the eutectic composition corresponding to the lowest eutectic temperature of 1233 K. The annealing temperature of 1223 K is quite close to this eutectic temperature. The similar possibility of liquid phase formation is expected also for the Zr–Fe system where the lowest eutectic temperature is about 1200 K for the Fe/Zr ratio of 24/76 [6]. On the other hand, for the Zr–Cr system, the lowest eutectic temperature is relatively high. It is about 1600 K for the Cr/Zr ratio of 22/78. Although the Zircaloy/Inconel reaction system cannot be simply explained by the binary phase diagrams, the analysis results suggests the possibility of a liquid formation at 1223 K.

The layer II consists of Ni, Cr, Fe, and quite a small amount of Zr (Table 2). Very small value of Zr concentration indicates the layer formed in the Inconel region, although concentration of Cr increased and that of Ni decreased from the initial composition of the Inconel.

3.1.2. Reaction at 1273 K

Fig. 4 shows cross-sections of the reaction couples annealed at 1273 K for various times. Thickness of the reaction layer increased with the lapse of isothermal annealing time. The growth of reaction layer is not uniform and it appears to be more remarkable at the bottom side. Decrease in the Zircaloy thickness at the bottom side after the annealing of 3.6×10^3 s was about 1.3 mm in average, while decrease in the Inconel thickness was only 0.2 mm. The Zircaloy was preferentially dissolved by the reaction with the Inconel, which was also reported by Hofmann et al. [7,8]. The microstructure of the reaction layer formed at the interface of the reaction couple annealed at 1273 K for 900 s is shown in Fig. 5. Two reaction layers, a thick layer I adjacent to Zircaloy and a thin layer II adjacent to Inconel, are seen in the figure. The layer I consists of bright precipitates and dark matrix, while the layer II consists of very fine structures. The double-layer structure was observed also in the samples annealed at 1323 K and 1373 K.

The average chemical composition of the reaction layers formed at 1273 K is shown in Table 2. The layer I consists mainly of Zr and Ni, and the composition is estimated to be $Zr_{0.72}Ni_{0.18}Cr_{0.04}Fe_{0.05}Sn_{0.01}$. The Ni/Zr atomic ratio of 20/80 is nearly the same as the eutectic composition at 1233 K in the Zr–Ni binary system (Fig. 3). The precipitate was identified as Zr_2(Ni, Fe), while the matrix was consisted mainly of zirconium. On the other hand, the composition of the layer II is analyzed to $Zr_{0.37}Cr_{0.34}Fe_{0.15}Ni_{0.07}$. The present analysis data for these layers agree quite well with that obtained by Hofmann et al. [7]. The formation of the double layers can be explained by the proposed mechanism by Hofmann et al. as follows. The layer I is the liquid phase formed by Zr–Ni and Zr–Fe eutectic reactions in the Zircaloy, and the layer II is the Cr-rich Zr(Cr, Fe)$_2$ phase formed by diffusion of Zr into the Inconel. The liquid phase formed in the layer I penetrates along the grain boundaries of the Zr(Cr, Fe)$_2$ phase

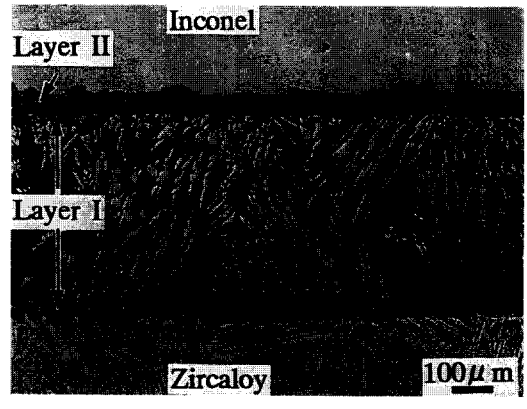

Fig. 5. Microstructure of the reaction layer of the reaction couple annealed at 1273 K for 900 s.

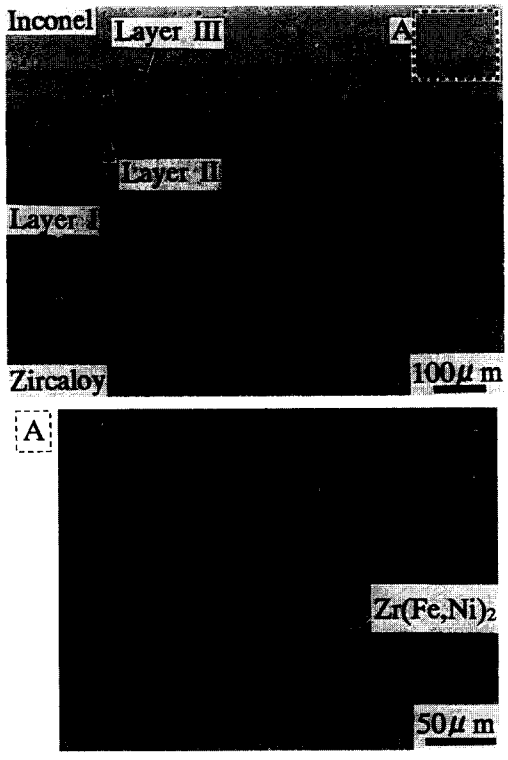

Fig. 6. Microstructure of the reaction layer of the reaction couple annealed at 1423 K for 180 s.

in the layer II and dissolves it. During cooling, the liquid phase decomposes into β–Zr and Zr_2(Ni, Fe) phase.

The composition of the layer I formed at 1223 K is different to some extent from that at 1273 K, although both layers have the same Ni/Zr ratio that is close to the eutectic composition of the Zr–Ni system at 1233 K. The average concentration of Cr in the layer I is considerably different from that at 1273 K, i.e., about 14 at.% for 1223 K and 4 at.% for 1273 K. Such a difference in the composition might affect the liquid phase formation in the Zircaloy/Inconel reaction.

3.1.3. Reaction at 1423 K

Fig. 6 shows the microstructure of the reaction layers formed at 1423 K for 180 s. The microstructure of the layers I and II is quite similar to those observed in the reaction couple annealed at 1273 K (Fig. 5). The similarity is evidenced by the result of the elemental analysis for the layers (Table 2). Specific features observed in this micro photograph are: (a) formation of another reaction layer (III) between the layer II and the Inconel, and (b) precipitation of a second phase, which is analyzed to be Zr(Fe, $Ni)_2$, in the Inconel region adjacent to the layer III. The composition of the layer III is analyzed to be $Zr_{0.07}Ni_{0.44}Cr_{0.21}Fe_{0.18}$. The formation of the Zr-rich layer (III) suggests another liquid phase formation at the Inconel side in this temperature range. Although the influence of Cr and Fe can not be neglected, the Zr–Ni binary phase diagram (Fig. 3) give a suggestion on the liquid phase formation. The diagram shows that the liquid phase can form in Ni–Zr alloy containing less than 15 at.% of Zr above 1443 K. The existence of Cr and Fe in Inconel might explain the temperature difference between the eutectic temperature of 1443 K in the Zr–Ni phase diagram and 1423 K.

Precipitation of the Zr(Fe, $Ni)_2$ phase in the Inconel was found on the grain boundary. The phase is considered to be formed by the preferential diffusion of Zr on the Inconel grain boundary. Such precipitates were observed also in the reaction couple annealed at 1473 K and 1523 K.

3.1.4. Reaction at 1473 K

Fig. 7 shows cross-sections of the reaction couples annealed at 1473 K for 30 to 120 s. As described, preferential dissolution of the Zircaloy was observed below 1373 K. On the other hand, dissolution of the Inconel is significant at this temperature. The melting temperature of Inconel is about 1600 K. Nevertheless, the original shape of

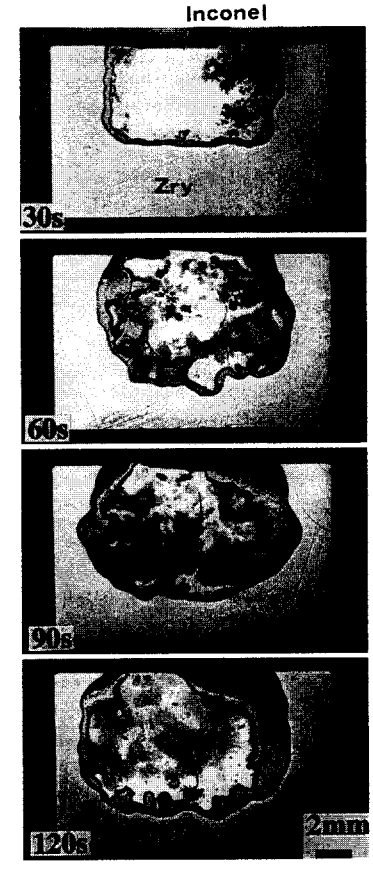

Fig. 7. Cross-sections of the reaction couples annealed at 1473 K for various times.

the Inconel pellet is completely lost after the annealing for 60 s. Fig. 8 shows the microstructure of the reaction layers in the sample annealed at 1473 K for 60 s. The region exhibiting the Widmannstätten structure at the right side is the intact Zircaloy and the bright and plain region at the left side is the intact Inconel. Various layers having different microstructures are observed between Zircaloy and Inconel. Four different phases represented by the regions 'A' to 'D' in Fig. 8 were analyzed with an SEM/EDX. The results are summarized in Table 2. The elemental composition of each phase is the mean value for the area surrounded by the dotted line in Fig. 8. The region 'A' exhibits the microstructure similar to the layer I formed at 1273 K (Fig. 5), and their chemical compositions are coincident with each other (Table 2). It shows that the Zr-rich liquid phase formation occurs at the Zircaloy side at the examined temperature from 1223 K to 1473 K. The analysis results show that Zr concentration sharply decreases from 68 at.% at region 'A' to 8 at.% at region 'D' and Ni concentration inversely increases from 19 to 47 at.% (Table 2). On the other hand, concentrations of Fe and Cr are not so much different in the region 'B' to 'C'. Therefore, interdiffusions of Zr and Ni can be regarded as the control process of the reaction. As seen in the phase diagram (Fig. 3), the Zr–Ni binary system has four eutectic points and the liquid phase can exist for a wide range of Ni/Zr ratio at temperatures above 1473 K. Consequently, a liquid phase having a certain gradient of the concentration of Zr or Ni appears to be formed between Zircaloy and Inconel at 1473 K. Observed resolidified phases with various microstructures are considered to form during the cooling process of the test. Ni-rich resolidified phase adjacent to the Inconel side can explain the significant dissolution of the Inconel by the possible eutectic formation at this temperature.

To investigate the elemental distribution in each resolidified phase, the boundary concentrations of four elements were analyzed for the reaction couples annealed at 1223, 1273, 1423, and 1473 K. The profiles of each element are shown schematically in Fig. 9. The narrow area (20–50 μm × 300–1000 μm) in the vicinity of each phase boundary was selected for the analysis. The layer I formed at 1273 K and the layer I and III formed at 1423 K show flat profiles of elemental concentrations. As previously mentioned, the layer I is the Zr-rich phase formed by eutectic reaction and the layer III is the Ni-rich phase. The layer II, solid layer, having low Ni concentration forms at the interface region with the Inconel at 1273 K, while it

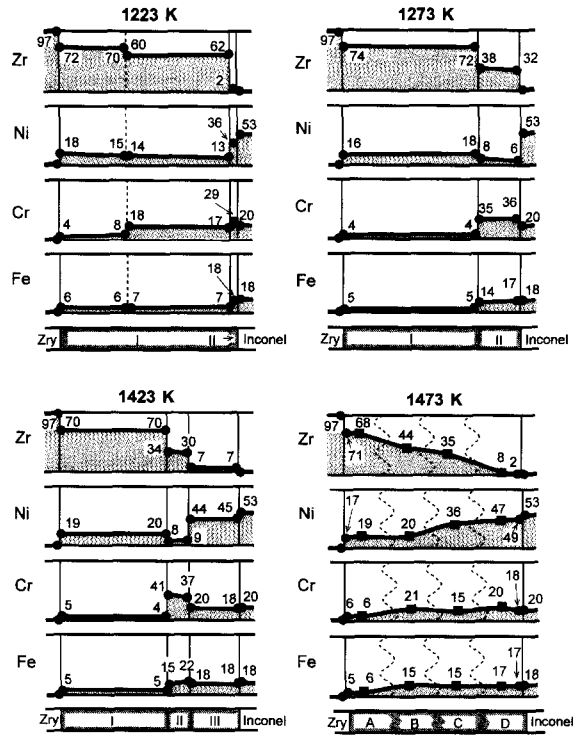

Fig. 9. Concentration profiles for different elements measured in the reaction layers of the reaction couples annealed at 1223, 1273, 1423, and 1473 K.

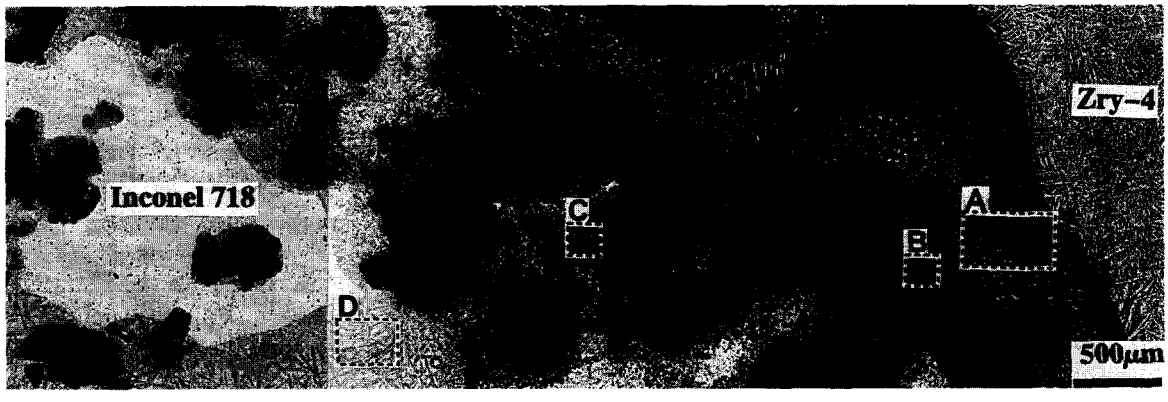

Fig. 8. Microstructure of the reaction layer of the reaction couple annealed at 1473 K for 60 s.

forms between two liquid phases, layer I and III, at 1423 K. For the reaction couple annealed at 1473 K, the boundary concentration between resolidified layer and Zircaloy or Inconel was measured, since the boundaries of each phase is not clear. The average concentrations measured on each phase having different microstructure are plotted in the figure in addition to the boundary concentrations. It is apparent that the concentrations of Zr and Ni gradually changed in the resolidified layer between Zircaloy and Inconel.

The obtained information on elemental distribution in reaction layers is essential for evaluating the reaction. García et al. [8] developed an interaction model to describe the Zircaloy/Inconel reaction at high temperatures. To determine the liquid diffusion coefficient, they estimated the maximum and the minimum concentration of Zr and Ni in the reaction layer from the solidus lines in the Zr–Ni binary phase diagram, since no experimental data on boundary concentration were available. The data obtained in the present study can provide rather reliable information to the analytical study of the actual reaction system between Zircaloy and Inconel.

3.2. Reaction kinetics

To evaluate the reaction rate, the decrease in Zircaloy crucible thickness at the bottom side and the decrease in Inconel pellet thickness was measured on the macro photographs of vertically cut cross-section of samples. The thickness of the reaction layer on the observed specific surface was not generally uniform. Then, the residual thickness of Zircaloy and Inconel was measured with an image analyzer and the average decrease in their thicknesses was obtained. Fig. 10 shows the correlation between decrease in Zircaloy thickness and square root of isothermal annealing time. Although some deviation is seen, a linear relationship is generally found at every test temperature. Therefore, the progress of the reaction can be described by a parabolic rate law. The calculated reaction rates are summarized in Table 3 and plotted as a function of the reciprocal temperature in Fig. 11. The reaction rates for decrease in the Zircaloy thickness discontinuously increased at two temperatures. The first increase occurred between 1223 K and 1248 K. The elemental analysis showed that the composition of the reaction layer formed at 1223 K was slightly different from that at high tempera-

Table 3
Reaction rate constants for decrease in the Zircaloy and the Inconel thickness

Temperature	Reaction rate constants (m^2/s)	
	decrease in Zircaloy thickness	decrease in Inconel thickness
1223 K	6.79×10^{-11}	2.55×10^{-12}
1248 K	3.84×10^{-10}	1.61×10^{-11}
1273 K	6.01×10^{-10}	3.13×10^{-11}
1323 K	1.80×10^{-9}	7.36×10^{-11}
1373 K	3.82×10^{-9}	1.04×10^{-10}
1423 K	7.99×10^{-9}	
1473 K	8.17×10^{-8}	
1523 K	1.37×10^{-7}	

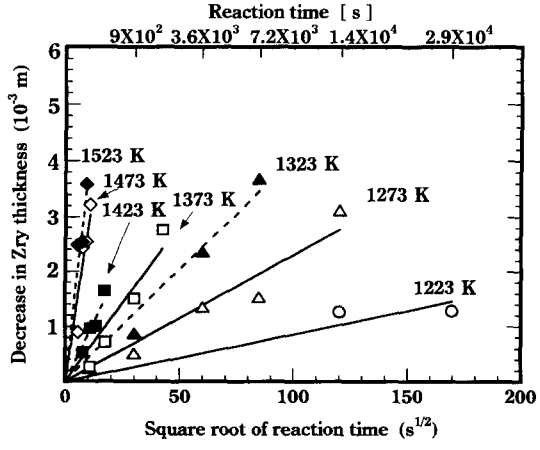

Fig. 10. Correlation between the decrease in the Zircaloy thickness and square root of the reaction time.

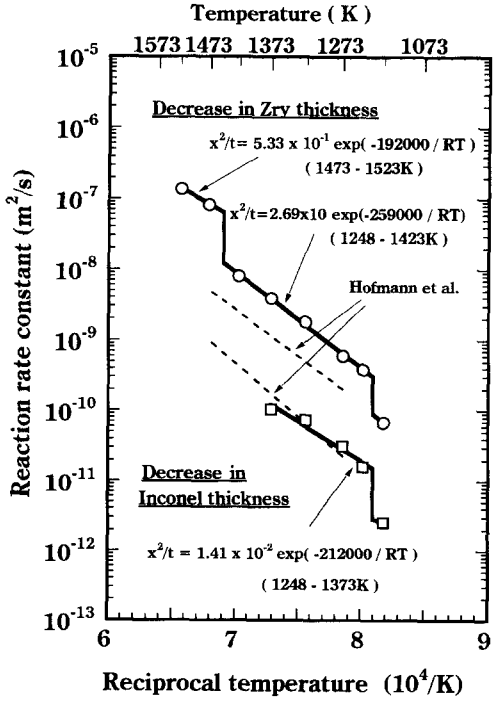

Fig. 11. Arrhenius plot of the reaction rate for the decrease in the Zircaloy of the Zircaloy/Inconel reaction.

tures. As mentioned in Section 3.1.1, the difference of composition may affect the liquid phase formation at this temperature level. The obvious discontinuity in the temperature dependence of the reaction rate suggests that the reaction mechanism is somewhat different from each other in the temperature range below and above about 1240 K.

Another discontinuity in the temperature dependence is seen between 1423 K and 1473 K. As shown in Fig. 9, the profile of elemental concentration is flat in each resolidified layer formed at 1273 K and 1423 K. On the other hand, in the resolidified layer formed at 1473 K that is above the temperature of discontinuity, the gradients of Zr and Ni concentrations are clearly seen. The gradient of Zr and Ni concentrations throughout the reaction layer at 1473 K indicates that the reaction was controlled by the interdiffusion of Zr and Ni in liquid phase. In contrast to this, the reaction at 1423 K was controlled by both liquid diffusion in layer I and III and solid diffusion in layer II. The diffusion coefficient in solid must be much smaller than that in liquid. Therefore, the rate determining step of the reaction at 1423 K can be considered to be the diffusion in layer II. Such difference of the reaction mechanism between 1423 K and 1473 K can explain the sudden increase of the reaction rate.

Consequently, two Arrhenius type rate equations for decrease in the Zircaloy thickness were derived separately for the two temperature ranges as follows:

$$x^2/t\ [\mathrm{m}^2/\mathrm{s}] = 2.69 \times 10 \exp(-259\,000/RT),$$

1248 to 1423 K,

$$x^2/t\ [\mathrm{m}^2/\mathrm{s}] = 5.33 \times 10^{-1} \exp(-192\,000/RT),$$

1473 to 1523 K,

where x is decrease in Zircaloy thickness, t is time, $R = 8.314\mathrm{J/mol\ K}$, T is given in K, and the activation energies in J/mol. Decrease in the Inconel thickness could not be measured precisely above 1423 K, since the Inconel pellet relocated remarkably from the original position or the complicated layer structures were formed in the Inconel at those temperatures. Then, a rate equation for decrease in the Inconel thickness was determined for the temperature range up to 1373 K as follows:

$$x^2/t\ [\mathrm{m}^2/\mathrm{s}] = 1.41 \times 10^{-2} \exp(-212\,000/RT),$$

1248 to 1373 K.

The reaction rate for decrease in the Inconel thickness at 1473 K is roughly estimated from the macro photograph shown in Fig. 7. The Inconel pellet of 5 mm thick was completely dissolved within 60 s. Assumption that the Inconel was completely dissolved for 60 s gives the reaction rate of about 8×10^{-7} m^2/s. This reaction rate is comparable to that for decrease in the Zircaloy thickness at the same temperature.

The data obtained by Hofmann et al. [7,8] are also plotted as a dotted line for comparison. Difference in the reaction kinetics is seen between the two data sets for dissolution of the Zircaloy. They obtained the lower reaction rates. The discrepancy can be attributed to the difference in both the experimental and the evaluation method employed in the two experiments. The heating rates of the experiments are different from each other. An electric resistance furnace was used in Hofmann's experiment and the heating rate was relatively low. Therefore, they started to count the isothermal annealing time when the temperature of a specimen reached 20 K below the predetermined annealing temperature [7]. In the present study, on the other hand, the holding time at the annealing temperature was accounted for the isothermal annealing time, since a rather higher heating rate of 10 K/s was achieved by the infrared furnace. Then, the same isothermal annealing condition experimented by us and Hofmann et al. does not mean the same temperature and holding time. In Hofmann's experiment, the reaction layer thickness was measured on the horizontal cross-section of the annealed reaction couple for evaluation of the reaction kinetics. As seen in Fig. 4, the reaction layer is thicker at the bottom side. Accordingly, the thickness of the reaction layer is considered to change with elevation. Therefore, they might obtain smaller reaction rates compared with our results from the measurement at the bottom side of the reaction couple.

The spacer grid made of Inconel is recently being replaced by that of Zircaloy in PWRs from the viewpoint of improving neutron economy. The replacement is preferable also for eliminating a possible source of low-melting-temperature eutectic formation in a fuel bundle during a severe accident.

4. Conclusions

To investigate the chemical interactions between Zircaloy-4 fuel cladding material and Inconel-718 spacer grid material during a severe accident in a PWR, the isothermal reaction tests were performed in the temperature range 1223 to 1523 K. As a result, the following conclusions were obtained.

- Multiple layers formed at the interface of the reaction couple.
- The reaction generally obeyed a parabolic rate law.
- Zircaloy was preferentially dissolved by the reaction with the Inconel below 1423 K, which is explained by a formation of Zr-rich eutectic.
- The dissolution of the Inconel became significant above 1473 K where Ni-rich eutectic formed.
- The discontinuities of the reaction rate constant was found at about 1240 K and about 1450 K. They could be correlated with the change of reaction mechanism at the corresponding temperature.
- The reaction rate equations for the decrease in the

Zircaloy thickness were determined for the temperature ranges as follows:

$x^2/t\ [\mathrm{m}^2/\mathrm{s}] = 2.69 \times 10 \exp(-259\,000/RT)$,
1248 to 1423 K,

$x^2/t\ [\mathrm{m}^2/\mathrm{s}] = 5.33 \times 10^{-1} \exp(-192\,000/RT)$,
1473 to 1523 K,

where x is decrease in Zircaloy thickness, t is time, $R = 8.314$J/mol K, T is given in K, and the activation energies in J/mol.

References

[1] D.A. Petti, Z.R. Martinson, R.R. Hobbins, C.M. Allison, E.R. Carlson, D.L. Hagrman, T.C. Cheng, J.K. Hartwell, K. Vinjamuri, L.J. Seifken, US Nuclear Regulatory Commission Report, NUREG/CR-5163, 1988.

[2] G. Schanz, S. Hagen, P. Hofmann, G. Schumacher, L. Sepold, J. Nucl. Mater. 188 (1992) 131.

[3] R.O. Gauntt, R.D. Gasser, L.T. Otto, Sandia National Laboratories Report, SAND86-1443, NUREG/CR 4671, 1989.

[4] P. Hofmann, U.S. Nuclear Regulatory Commission Report, NUREG/CR-5119, 1988.

[5] S.M. Jensen, D.W. Akers, B.A. Pregger, OECD LOFT-T-3810, 1989.

[6] T.B. Massalski, Binary Alloy Phase Diagrams, 2nd Ed. American Society for Metals, Metals Park, OH, 1990).

[7] P. Hofmann, M. Markiewicz, Kernforschungszentrum Karlsruhe Report, KfK 4729, 1994.

[8] E.A. Garcia, P. Hofmann, A. Denis, J. Nucl. Mater. 189 (1992) 20.

[9] M.R. Warren, K. Rorbo, E. Adolph, J. Nucl. Mater 58 (1975) 185.

[10] F. Nagase, T. Otomo, H. Uetsuka, T. Furuta, Japan Atomic Energy Research Institute Report, JAERI-M 90-165, 1990.